

CLOUD CHAMBER STUDIES IN COSMIC RAYS

AT AN ALTITUDE OF 30,000 FEET

Thesis by

Raymond Voiles Adams, Jr.

In Partial Fulfillment of the Requirements for the Degree  
Doctor of Philosophy

California Institute of Technology  
Pasadena, California  
1948

### ACKNOWLEDGEMENT

This research was supported in part by the Office of Naval Research through Contract N6onr-102 Task Order No. III with the California Institute of Technology, and in part by the National Research Council through the grant of a Predoctoral Fellowship.

The construction of the apparatus, and its operation under the trying conditions of high altitude flight and the rigors of life at Inyokern were shared with Dr. Paul E. Lloyd and Mr. R. Ronald Rau, without whom these data could not have been obtained. I wish to thank Mr. Aaron J. Seriff for his aid in measuring the photographs. I am also indebted for the willing cooperation of the many officers and men of the U. S. Air Forces, of the Naval Ordnance Test Station at Inyokern, and of the Office of Naval Research who participated in the operational part of the project. In particular, it is a pleasure to acknowledge the untiring work of Staff Sergeant David Burns, crew chief of B-29 No. 521857.

In conclusion, the writer wishes to express his deep appreciation to Professor Carl D. Anderson for his guidance, his continued interest, and his many helpful discussions.

## ABSTRACT

Cloud chamber observations of cosmic rays have been made in a B-29 aircraft, flying at altitudes of 30,000 ft. A 17-cm cloud chamber in a magnetic field of 7500 gauss was employed. From curvature measurements on 245 cloud tracks, the energy spectrum of cosmic rays at 30,000 ft has been determined. In contrast to the roughly equal numbers of positive and negative particles which are found at sea level, the high altitude data show that positive particles dominate the negative particles by a ratio of 2:1. The different forms of the positive and negative spectra show that there exists among the positives a type of particle which is not represented among the negatives. The data are consistent with the hypothesis that these positives are protons, measured energies of which extend to 2.5 Bev. At least three-fourths of the protons probably are secondary particles. The remainder may well come directly from a primary proton component.

P U B L I C A T I O N S

On the Mass and the Disintegration Products of the Mesotron,

Carl D. Anderson, Raymond V. Adams, Paul E. Lloyd, and

R. Ronald Rau, Phys. Rev. 72, 724 (1947)\*

Cosmic Rays at 30,000 Feet, Raymond V. Adams, Carl D. Anderson,

Paul E. Lloyd, R. Ronald Rau, and Ram C. Saxena, Rev. Mod. Phys.,

(Spring, 1948)\* /

\* Reprints are not yet available.

/ This paper contains the material discussed in this thesis.

## T A B L E   O F   C O N T E N T S

<u>SECTION</u>	<u>TITLE</u>	<u>PAGE</u>
I	Introduction	1
II	Historical Discussion	2
III	The Apparatus	3
IV	The Energy Spectrum	7
V	Discussion of Results	21
	References	30
 <u>APPENDIX</u>		
A	Previous Experiments	32
B	Electronic Equipment Diagrams	42
C	Method for Curvature Measurements	47

## I. INTRODUCTION

Herein is described a study of the energy spectrum of cosmic rays at an altitude of 30,000 ft (9200 m) above sea level. The energy spectrum was determined by direct measurement of the curvatures of individual rays in the magnetic field of a Wilson cloud chamber. The cloud chamber was carried aloft in the pressurized cabin of a U. S. Air Forces B-29 aircraft, which had been converted into a flying laboratory under the auspices of the Office of Naval Research. The construction and operation of the apparatus was carried out under the direction of Professor Carl D. Anderson and in cooperation with Dr. Paul E. Lloyd and Mr. R. Ronald Rau.

This paper is divided into sections which describe research in cosmic ray energies carried out by other research workers, the cloud chamber and its related equipment, the experimental data, and the implications of the data. Appended are diagrams of the electronic equipment and a discussion of the method used in data reduction together with critical remarks on the limits of validity of the measurements.

## II: HISTORICAL DISCUSSION

Clouds were first produced in an expansion chamber by C. T. R. Wilson in 1895.<sup>(1)</sup> Curiously, Wilson's experiment was inspired by a desire to produce in the laboratory cloud phenomena such as he had observed in nature. In the following year Wilson studied the effect of the degree of supersaturation (produced by the degree of expansion) on the cloud formation, and first observed the production of clouds on ions produced by Röntgen rays. By 1911 Wilson obtained photographs of alpha- and beta-rays by introducing an electric "sweep" field to remove old ions from his chamber. The Wilson chamber was subsequently applied to the study of radioactive processes by many research workers. It was not until 1929 that cosmic radiation was observed and recognized as such in a cloud chamber by Skobelzyn.<sup>(2)</sup> The cloud chamber has since been used by many workers in the field of cosmic radiation. Numerous improvements such as the vertical chamber, the application of very strong magnetic fields, and the introduction of Geiger tube control have made the instrument a more valuable research tool.

In 1932, 1933, and 1934,<sup>(3)</sup> Anderson reported energy

measurements on cosmic rays with a vertical Wilson chamber placed in a magnetic field of 17,000 gauss. In 1933 Kunze<sup>(4)</sup> reported his measurements of the sea level spectrum. In 1937 Blackett<sup>(5)</sup> published the results of a very careful study of the sea level energy spectrum, measuring energies up to 20 billion electron-volts and showing the existence of even more energetic particles. Other sea level energy measurements were reported by Leprince-Ringuet and Crussard in 1937,<sup>(6)</sup> Jones in 1939,<sup>(7)</sup> and Hughes in 1940.<sup>(8)</sup> In 1946 Powell<sup>(9)</sup> reported measurements of cosmic ray energies at an altitude of 14,000 ft using lead plates inside his cloud chamber in lieu of a magnetic field. Cloud chamber experiments at an altitude of 29,000 ft were reported by Herzog and Bostick in 1941,<sup>(10)</sup> but due to the fact that a magnetic field of but 700 gauss was used, the measurements can be considered only as qualitative.<sup>(11)</sup>

### III. THE APPARATUS

The cloud chamber and electromagnet used in these experiments was built by Dr. Anderson in 1930<sup>(3)</sup> for the purpose of studying cosmic ray energies. In the following years the apparatus was used in extensive investigations into the nature

of cosmic rays at Pasadena, in Panama, and on Pikes Peak. For the work here described only the electromagnet and the basic mechanical parts of the cloud chamber were used, the automatic control equipment being built especially for operation in the airborne laboratory. The high altitude data will be compared with Dr. Anderson's sea level data, a valid comparison in that the shielding of the cloud chamber, which affects the shape of the energy spectrum, is the same.

Designed to operate automatically, the apparatus worked very satisfactorily under the difficult problems encountered in the airborne laboratory. The presence of an operator to make minor but essential adjustments was necessary. Much of the ease of operation can be attributed to the fact that the control equipment was designed to operate in the bombbay of the aircraft, where low atmospheric pressures and sub-zero temperatures prevail, whereas actually the cloud chamber was installed in the after pressurized compartment, where the pressure was about  $2/3$  of an atmosphere and the temperature was about 20 deg C.

The cloud chamber, 17 cm in diameter and 2 cm deep, is of the reciprocating-piston type. It is placed vertically between the pole pieces of the electromagnet, which in the

airplane was operated with a field intensity of 7500 gauss, uniform to within 10 per cent throughout the chamber region. The chamber expands when a solenoid-operated mechanism releases the piston, permitting it to move under the air pressure differential between its faces. Argon gas, with ethyl alcohol vapor, at a total pressure of 1.7 atmospheres is used in the chamber, while a pressure of about one-half an atmosphere is maintained behind the piston. Compressed air resets the piston. The cloud chamber expansion is completed in approximately 4 milliseconds after the passage of the ray, producing very sharp tracks.

A camera, its optic axis parallel to the magnetic field, photographs the tracks through a hole in one pole piece of the magnet. Mirrors placed vertically on the sides of this hole produce two lateral views of the tracks, permitting stereoscopic examination of tracks. Only the direct view of the chamber is used for curvature measurements. The camera has a 2-inch f/2 Taylor-Hobson-Cooke lens. The tracks are illuminated by light from a General Electric FT-27 flash tube, the flash duration time determining the exposure of the film. The tracks are recorded on 35 mm Eastman Linagraph Ortho film. This film was found to have greater contrast and speed than films such as Eastman Super-XX and Ansco Ultraspeed.

The chamber expands on the coincidence of pulses from two Geiger-Meuller tubes, one placed above the chamber and one below. The pulse from each tube is amplified and sharpened in a Neher-Harper stage, and the two resulting pulses are mixed in a conventional Rossi stage.\* The coincidence pulse is amplified and greatly sharpened in a blocking oscillator stage before it triggers a thyratron. The latter initiates a high voltage, condenser discharge through the release solenoid, releasing the chamber piston. A motor-driven timer controls the cycle of operations which reset the apparatus for each succeeding photograph. A second timer introduces a fixed time delay of about 45 sec between expansions to permit the chamber to reach thermal equilibrium following the compression of the gas.

The principal source of error in cloud track measurements lies in distortions of the tracks produced by mass motion of the gas within the chamber. Because temperature gradients within the chamber produce such mass motion, it is necessary to maintain the chamber temperature constant and uniform during operation. The chamber temperature is determined by that of the iron and copper at the center of the magnet.

\* Appendix B shows diagrams of this electronic equipment.

Because of its large mass the latter follows the temperature of its surroundings only very slowly; hence, temperature equilibrium must be established by refrigeration or heating of the cabin for many hours before flight. During flight the magnet temperature, and hence that of the chamber, is determined by the temperature of the cooling water, which circulates through the magnet coils. The water temperature can be controlled so that the temperature of the chamber remains constant to  $\pm 1^{\circ}$  C throughout a flight. As a result, tracks obtained at 30,000 ft are found to be as free of distortion as those photographed in a surface laboratory.

#### IV. ENERGY SPECTRUM -- THE EXPERIMENTAL DATA

Magnetic curvature measurements on the cloud tracks of 245 cosmic ray particles are presented below. The choice of tracks to be measured was made so as not to influence the distribution in energy of the particles which occur singly. From among the data taken on three flights all tracks which occurred singly and which were at least 8 cm long were measured. After the measurements had been made all the tracks occurring in the last half of the data from one flight were eliminated because

the higher energy tracks seemed to be unduly distorted.

The curvatures of all tracks of radii less than 140 cm were measured by direct comparison of the projected tracks with a family of circular arcs. The curvatures of all other tracks were measured with a comparator by the method described in Appendix C.

For low momentum tracks the accuracy of the measurements is limited by the inhomogeneity of the magnetic field, while for high momentum tracks the accuracy of measurement is limited by distortions produced by mass motion of the gas within the cloud chamber. Since the magnetic field is homogeneous to about 10 per cent, the accuracy of measurements of momenta up to  $2 \times 10^6$  gauss-cm is about 10 per cent. Above this momentum the accuracy of measurements decreases. The measurements of  $5 \times 10^6$  gauss-cm are accurate to  $\pm 20$  per cent; of  $7 \times 10^6$  gauss-cm,  $+40$  per cent,  $-30$  per cent; of  $11 \times 10^6$  gauss-cm,  $+100$  per cent,  $-40$  per cent. For higher momentum tracks, uncertainties in the curvature measurements permit only the placing of a lower limit of  $1.5 \times 10^7$  gauss-cm on the momenta.

Of the 245 tracks, 206 are classified as counter-controlled tracks and 39 as random tracks. "Random" particles

are those which can not have tripped the chamber either because the positions of their tracks in the chamber preclude the possibility of their passing through both counters or because their extreme sharpness shows they have passed through the chamber after the expansion has taken place. (Tracks occurring prior to counter-actuation are not included because they lack the sharpness necessary for accurate measurement.) All other tracks are called "counter-controlled" tracks. Among the latter are probably a few tracks which entered the chamber before or after the expansion, but whose sharpness is not noticeably different from that of a counter-controlled track. It is presumed that the number of such tracks is too small to affect the energy distribution appreciably.

All tracks of measurable curvature are classified according to sign of electric charge. The sign of the charge of a cosmic ray particle is uniquely determined by its direction of curvature in a magnetic field, provided that the direction of travel of the particle is known. For the tracks here reported the direction of the magnetic field is such that positive tracks curve clockwise while negative tracks curve counterclockwise. Because it is impossible to tell the direction of travel of the particles, but since it is known that most cosmic ray particles are traveling downward, it is assumed for purposes of classification

that all the particles are moving downward. All particles are taken to be singly charged.

All tracks are classified as to whether their specific ionization is equal to or greater than the minimum ionization for a singly-charged particle. Inasmuch as these tracks are quite sharp, the single ions along the tracks are not resolved, and an accurate ion count is impossible. Since the eye is unable to distinguish the density of a sharp track which has less than 3 to 4 times the minimum ionization from the density of a track of minimum ionization, the classification "greater than minimum ionization" implies an ionization greater than 3 to 4 times the minimum. The classification "minimum ionization" may imply an ionization almost as great as 3 to 4 times the minimum. Figs. 1 and 2 show representative tracks of the same momentum, one of which has greater than minimum ionization while the other has minimum ionization. The first particle is a proton, and the second is either a mesotron or an electron.

Because the magnetic curvature measures the momentum rather than the energy of the particle, the "energy" distributions are given in terms of the magnetic curvature,  $H\rho$ , in gauss-cm. Tables I and II list the momenta of all positive and negative particles. Table III lists the particles which are unclassified

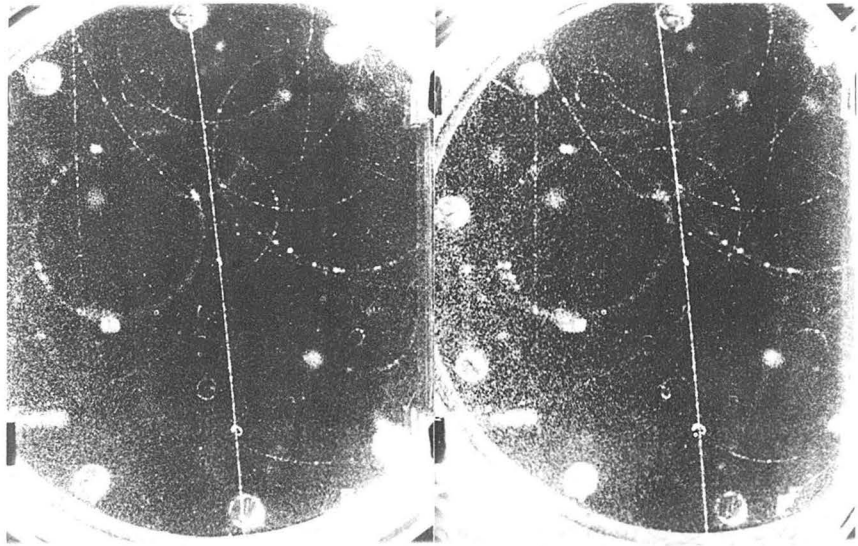


Fig. 1 This is an example of a proton of magnetic curvature  $1.6 \times 10^6$  gauss-cm. A proton of this momentum has an energy of 110 Mev, an ionization of 3.2 times the minimum, and a range of 11 gm/cm<sup>2</sup> in air.

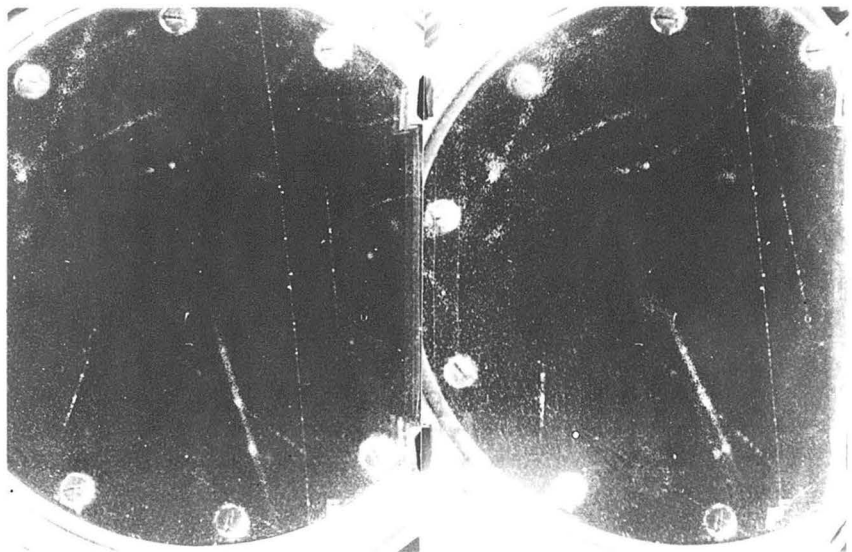


Fig. 2 This is a track of minimum ionization, which is shown for comparison with Fig. 1. Because its magnetic curvature also is  $1.6 \times 10^6$  gauss-cm, it must be either an electron or a mesotron, either of which should exhibit minimum ionization at this momentum.

TABLE I All Positive Particles

Magnetic Curvature in Gauss-Cm for Each Particle

* 3.2 x 10 <sup>4</sup>	6.8 x 10 <sup>5</sup>	1.5 x 10 <sup>6</sup>	2.0 x 10 <sup>6</sup>	3.2 x 10 <sup>6</sup>	5.6 x 10 <sup>6</sup>
* 3.7	# 7.5	1.5	2.0	3.5	5.6
* 9.5	* 7.5	# 1.6	* 2.1	3.5	5.6
* 1.05 x 10 <sup>5</sup>	* 8.2	# 1.6	2.1	3.8	6.4
* 1.3	* 8.7	1.6	2.2	3.8	6.4
1.35	# 8.7	1.6	2.2	3.8	* 6.4
1.7	9.3	1.6	2.2	3.8	7.5
1.95	9.4	1.6	2.2	3.8	7.5
* 2.5	9.5	1.6	2.2	3.8	7.5
2.6	9.8	1.6	2.3	3.8	7.5
2.8	* 1.0 x 10 <sup>6</sup>	1.7	2.4	* 4.1	7.5
3.0	# 1.0	1.7	2.5	4.5	7.5
3.2	1.0	1.7	2.5	4.5	7.5
* 3.5	# * 1.05	1.7	2.6	4.5	7.5
* 3.5	* 1.05	1.7	2.6	4.5	7.5
3.6	1.05	1.7	2.6	4.5	9.0
3.6	1.1	1.8	2.8	4.5	9.0
3.8	1.1	1.9	2.8	4.5	1.1 x 10 <sup>7</sup>
4.1	# 1.3	1.9	2.8	5.0	1.1
4.4	# 1.3	1.9	2.8	* 5.6	1.1
* 4.9	# * 1.4	1.9	3.0	5.6	1.1
4.9	# * 1.4	1.9	3.2	5.6	1.1
* 6.0	# * 1.5	1.9	3.2	5.6	1.1
6.5	1.5	* 2.0	3.2	5.6	1.1

\* Random particles # Ionization greater than minimum

TABLE II All Negative Particles

Magnetic Curvature in Gauss-Cm for Each Particle

	4.5 x 10 <sup>5</sup>	1.7 x 10 <sup>6</sup>	3.8 x 10 <sup>6</sup>
* 3.8 x 10 <sup>4</sup>	4.9	* 1.9	4.1
* 5.4	5.4	1.9	4.1
* 5.6	6.5	1.9	4.1
* 6.6	7.3	1.9	4.1
* 9.6	7.8	2.0	5.0
1.1 x 10 <sup>5</sup>	9.0	2.4	5.6
1.25	9.2	2.5	5.6
1.4	1.05 x 10 <sup>6</sup>	2.5	5.6
* 1.95	1.1	* 2.8	5.6
1.95	1.2	2.8	5.6
2.0	1.25	3.0	7.5
2.8	1.3	3.0	7.5
* 3.2	1.3	3.2	9.0
3.3	1.4	3.2	9.0
4.1	1.4	3.8	1.1 x 10 <sup>7</sup>
4.1			

\* Random Particles

TABLE III Particles Unclassified

as to Sign of Charge

Magnetic Curvature in Gauss-Cm for Each Particle

2.7 x 10 <sup>4</sup>	1.8 x 10 <sup>5</sup>
3.6 x 10 <sup>4</sup>	1.9 x 10 <sup>6</sup>
3.7 x 10 <sup>4</sup>	5.0 x 10 <sup>6</sup>
6.6 x 10 <sup>4</sup>	1.1 x 10 <sup>7</sup>

TABLE IV Total Numbers of Particles

	Positive	Negative	High Momentum
All particles	142	64	31
Counter-Controlled Particles	120	55	31

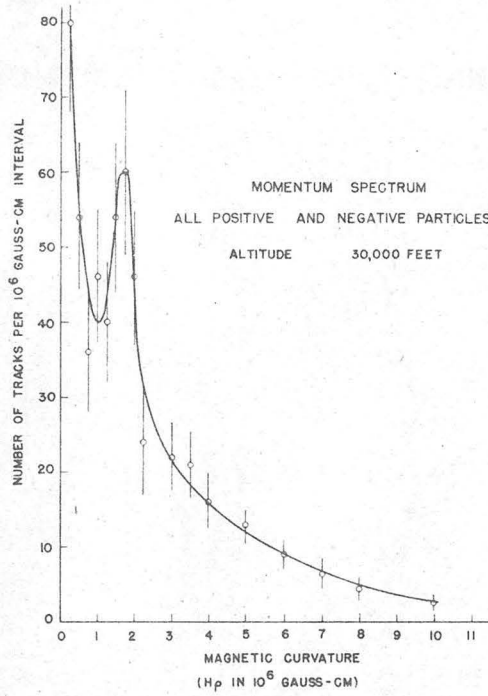


Fig. 3 Spectrum of All Particles

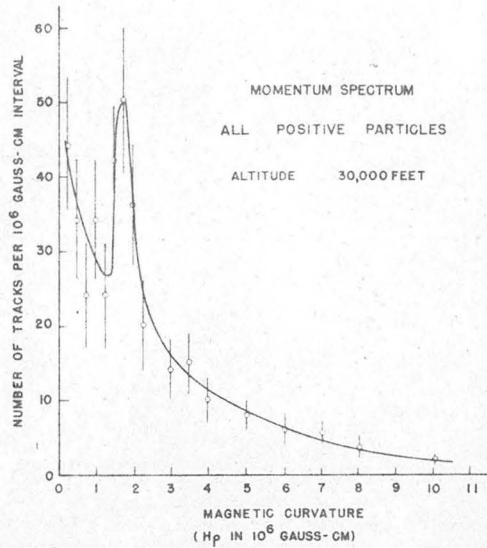


Fig. 4 Spectrum of All Positive Particles

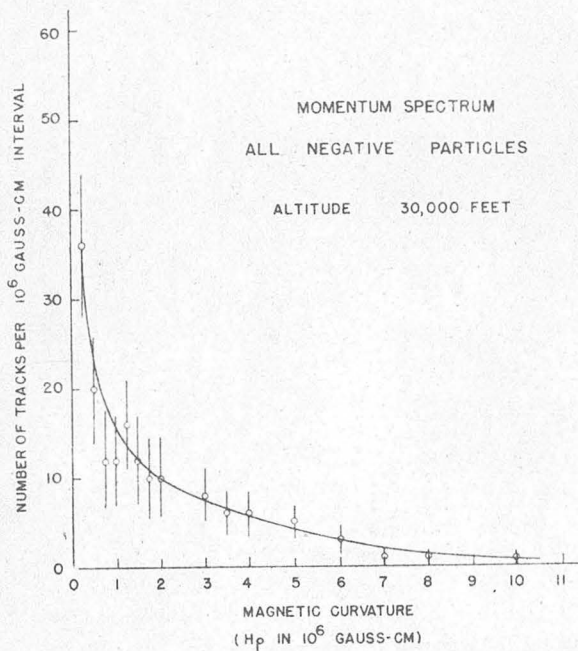


Fig. 5 Spectrum of All Negative Particles

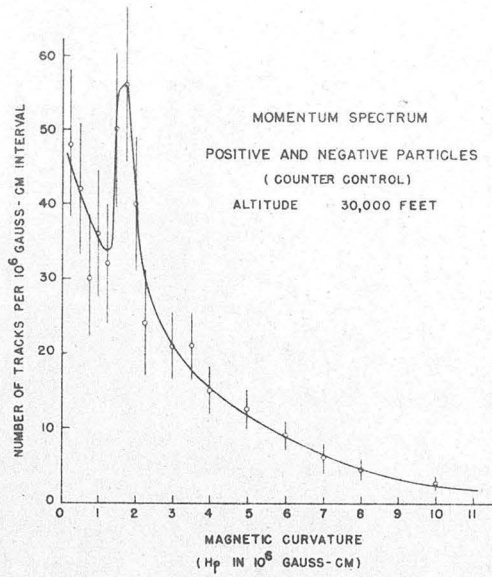


Fig. 6 Spectrum of All Counter-Controlled Particles

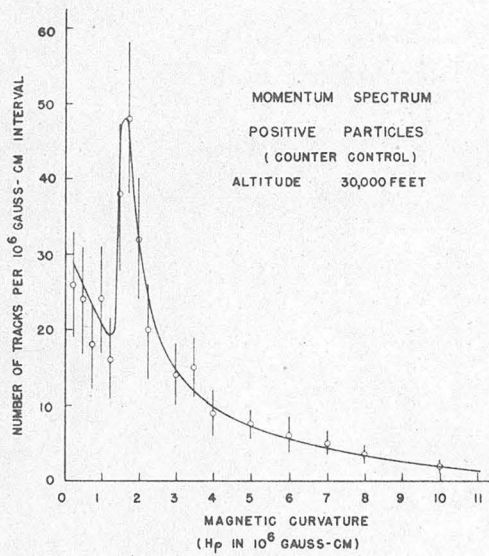


Fig. 7 Spectrum of Positive Counter-Controlled Particles

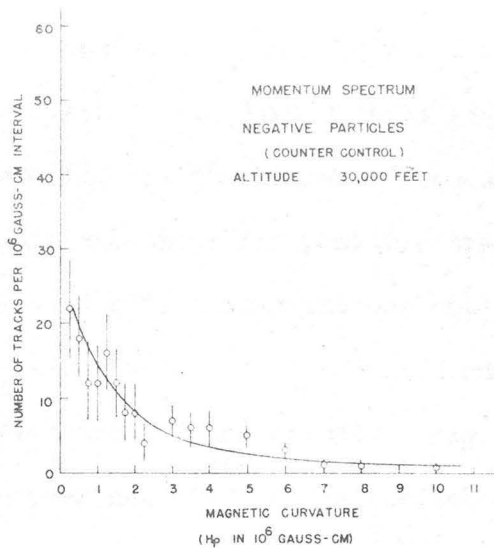


Fig. 8 Spectrum of Negative Counter-Controlled Particles

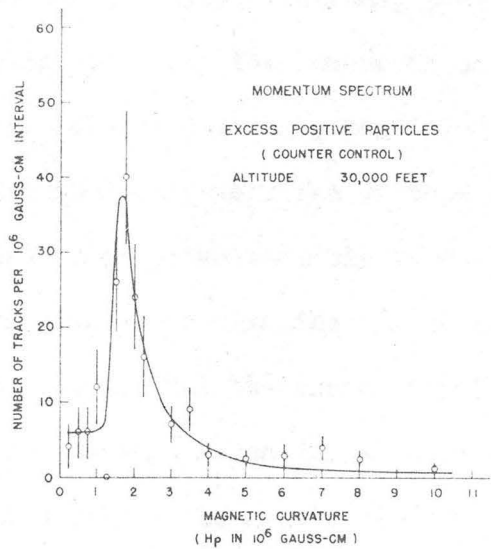


Fig. 9 Spectrum of Excess Positive Particles

as to sign of charge. Table IV gives the total numbers of particles of each sign. Fig. 3 shows graphically the momentum distributions for all tracks regardless of sign. Figs. 4 and 5 show the distributions for positive tracks and for negative tracks, respectively. These include both counter-controlled tracks and random tracks. Figs. 6, 7, and 8 show similar curves for counter-controlled tracks only. Fig. 9 shows the excess of positive over negative tracks for the counter-controlled group.

The momentum distribution includes in the main the following particles: mesotrons (positive and negative), protons, and a few single electrons, the latter probably occurring principally at the low-momentum end of the distribution. Because these data include only particles which occur singly, it is assumed that only very few of them are shower electrons. The fact that no negative particle is found to have an ionization and momentum consistent with the  $e/m$  of a proton can be taken as evidence, first, that the assumption that nearly all particles are traveling downward is valid, since a positive proton traveling upward would appear to be negatively charged, and second, that negative protons do not occur (in thus-far detectable numbers) at 30,000 ft altitude.

The following experimental results are evident from the data: (1) positive tracks are much more numerous than negative tracks;\* (2) the positive and negative spectra are quite dissimilar; and (3) a number of tracks ( $11 \pm 3$  per cent of the total number) have momenta greater than  $1.5 \times 10^7$  gauss-cm and cannot be classified as to sign of charge.

In the momentum range  $(2 \text{ to } 10) \times 10^6$  gauss-cm both positive and negative particles decrease in numbers in much the same fashion. Although it cannot be said (because of statistical uncertainties) that the numbers decrease according to any mathematical law, the experimental data are consistent with an energy power law,  $kE^{-\gamma}$ , where  $\gamma$  equals 1.3 for negative particles and 1.5 for the excess positive particles.\*\* A much more rapid decrease ( $\gamma$  equals 2.8) is usually predicted for the particles of higher energies (above 7 Bev).

\* This large positive excess is confirmed by a second set of photographs which were taken at 30,000 ft with the magnetic field reversed.

\*\* The solid curves of Figs. 8 and 9 are drawn according to this power law.  $k$  and  $\gamma$  were chosen by the standard least-square deviation method.

## V. DISCUSSION OF RESULTS

The experimental data of various research workers\* show that the cosmic ray particles that occur singly at sea level have the following properties: (1) the numbers of particles decrease fairly rapidly with increasing energies, (2) positive and negative particles occur in about the same numbers, the positive excess being only about ten per cent of the total number of particles, (3) the shape of the energy distribution curve for positive particles is similar to that for the negative particles, and (4) particles identifiable as protons are extremely rare. Almost all of the singly-occurring particles at sea level are believed to be mesotrons, and so according to the above, positive and negative mesotrons have similar spectra.

Very few energy distribution data are available for altitudes of the order of 14,000 ft. Measurements on a group of 48 tracks\*\* show a positive-to-negative particle ratio of 1.8 at Pikes Peak, indicating that there may be a rather large positive excess at that altitude. Further, there do occur at this altitude a number of protons, but the per cent of all particles which are protons has not been determined.

\* Appendix A carries a detailed discussion of these data.  
\*\* Unpublished data of C. D. Anderson and S. H. Neddermeyer.

The presence of a large excess of positive particles at 30,000 ft shows a marked change in the characteristics of cosmic radiation between this altitude and sea level. Although the 14,000 ft data are meager, there is an indication that this change may be much smaller between 14,000 ft and 30,000 ft than it is between sea level and 14,000 ft.

The dissimilarities in the positive and negative spectra at 30,000 ft show that there exists among the positive particles a component which has no symmetric counterpart of negative charge. If one assumes that positive and negative mesotrons exhibit the same symmetry at 30,000 ft as at sea level, the negative spectrum of Fig. 8, which probably consists principally of mesotrons, can be taken to represent also the spectrum of positive mesotrons. The positive excess of Fig. 9 will then represent another type of particle.

The data are consistent with the interpretation that the positive excess consists principally of protons. Supporting this hypothesis are the following: first, identifiable protons constitute 30 per cent of the positive particles in the momentum range  $(0.4 \text{ to } 1.6) \times 10^6$  gauss-cm, a range in which protons are distinguishable from other particles; and second, the positive excess spectrum shows a relatively sharp cut-off at about

$1.2 \times 10^6$  gauss-cm, which is the minimum momentum which a proton must have to penetrate the material between the chamber and the lower Geiger tube to produce a coincidence. (The greater portion of the identifiable protons are not among the counter-controlled tracks because the proton cut-off occurs in the region of momenta where protons have about 2 to 4 times the minimum ionization.)

These data are the first direct indication that protons of energies as great as 1 to 2 Bev exist in abundance at high altitudes. It is well known that protons of low energy are a component of cosmic radiation which are produced in nuclear disintegrations and in knock-on collisions of neutrons with nuclei. Photographic emulsion experiments<sup>(12,13)</sup> show these protons to be most abundant in the energy range 5 to 30 Mev, with some having energies up to 80 Mev. (Such experiments can not detect protons of energies much higher than this value.)

Cloud chamber experiments do not, of course, identify the origin of a particle as primary or secondary because all particles of a given type and given energy look the same. A reasonable guess as to their source must be made with the use of other considerations.

At first thought one is tempted to assign only a secondary

origin to the high energy protons. Supporting reasons are:

(1) many low energy protons are observed directly to be the result of secondary processes; (2) the intensity of low energy protons increases with altitude at about the same rate as does the intensity of the secondary, soft radiation, indicating that the protons may be produced by the soft radiation; and (3) if the primary particles are indeed protons, one would not expect them to penetrate to the 30,000 ft level, above which there is 300 gm/cm<sup>2</sup> of air.

These reasons should be examined more closely. The first two reasons concern low energy protons (energies less than 80 Mev), and so one may, if necessary, disregard them as not relevant to a discussion of high energy protons (energies between 0.2 and 2 Bev). For the basis of the third reason, the following is quoted from Heisenberg (1941):<sup>(14)</sup> the "primary proton spectrum is apparently strongly absorbed in the atmosphere since, at the greatest heights where protons have thus far been sought, only a relatively weak proton component has been found." Thus one must not expect to find primary protons in the lower atmosphere because high energy protons have not been found at those altitudes! The new evidence indicates that, on the contrary, high energy protons are indeed present, and so this reason must be discarded.

There are then no definite a priori reasons to suppose that the high energy protons which are found at 30,000 ft do not consist, at least in part, of primary particles. An examination of the primary proton hypothesis can perhaps be of value in the formation of more definite conclusions.

It has been postulated that the primary radiation consists largely of protons.<sup>(15,16)</sup> The basic experimental reasons for the hypothesis are (1) the primary rays which are sensitive to the earth's magnetic field are of positive charge, as is indicated by the east-west assymetry of the total sea level radiation; and (2) all known, positively charged particles other than protons are ruled out as primary particles on experimental grounds. The mesotrons of the penetrating component, which is increasing in intensity at the highest altitudes at which experiments have been made, cannot be primary particles because mesotrons are known to undergo radioactive decay with a half-life of about 2 microseconds, and so cannot exist for great distances in free space. Furthur, the mesotrons cannot be produced by a primary electron (or photon) component because electron showers are not observed at the very high altitudes where the penetrating component is still increasing.<sup>(16)</sup>

The conversion of the primary particles into mesotrons

must be very rapid at the top of the atmosphere in order that the altitude-intensity curve of the penetrating component be explained. In order that the cross-section for the mesotron production process be not unreasonably large, the process has been postulated to be a multiple one; i.e., a very high energy proton encounters a nucleus and gives up its energy in the production of several mesotrons in a single act. The multiplicity should be about 9 for protons of energies above 7 Bev, decreasing to about 3 or 4 for energies as low as 3 Bev. The process should not occur frequently for somewhat lower energies. <sup>(17)</sup>

It has been customary to say that the primary proton loses all its energy in the mesotron production process because protons have not been observed in numbers at high altitudes before, although it has been recognized that several low energy nucleons may be ejected. Since high energy protons have now been found at altitude, it is not unreasonable to suppose that a primary proton, while giving up the larger share of its energy in the creation of mesotrons, may survive the process\* with an

\* If the cross-section for multiple mesotron production is of the order of nuclear dimensions, as seems to be necessary for an explanation of the experimental data, then primary protons can be expected to knock out of nuclei by direct impact nucleons of very high energy. Protons from this source could not, of course, be distinguished from primary protons which have lost only a part of their energy in traversing a nucleus. The remaining discussion can apply equally well to any high energy protons left over after the first impacts of the primary particles with nuclei.

energy as large as 2 to 2.5 Bev. Because the multiple process probably does not occur for energies much below 2 to 3 Bev, protons of lower energies should penetrate into the atmosphere, losing their energy principally by ionization. The residual range of a 0.9 Bev proton is about  $300 \text{ gm/cm}^2$  so that all protons of lower energy would not survive down to an altitude of 30,000 ft. A 2.5 Bev proton has a residual range of about  $1000 \text{ gm/cm}^2$  and so can reach the 30,000 ft level with a residual energy of about 1.7 Bev. Further, such a proton can just reach sea level.

The following description is, then, consistent with the observations. A primary proton component produces the mesotron component by a multiple process. There remains from the process an appreciable number of protons of energies up to about 2.5 Bev. These presumably are incapable of multiple mesotron production. Those protons having energies in the range 1 to 2.5 Bev survive to the 30,000 ft level and constitute a part of the protons there observed. A few of these protons penetrate to the 14,000 ft level, and essentially none penetrate to sea level.

It should be noted that the observed scarcity of cosmic ray protons at sea level requires that there be no protons of energies greater than about 2.5 to 3 Bev in the top of the

atmosphere, unless they lose energy through some process other than ionization. This difficulty is, of course, taken care of by the mesotron production process, which on other grounds is postulated to occur at greater energies.

It will be recalled that the data indicate that as many as 30 per cent of the particles at 30,000 ft are protons. To account for such a large proportion of the particles on the assumption that they all are primary protons seems difficult. If a primary proton component produces a mesotron component with an average multiplicity of 9, and if an average of only one energetic proton is left from each process, the remaining proton component can be only of the order of ten per cent of the mesotron-proton component. (This proportion will be changed somewhat by the time that the particles reach the 30,000 ft level because of probable differences in the initial proton and mesotron spectra, because some of the mesotrons are lost by the decay process, and because the penetrating powers of a proton and a mesotron of the same energy differ somewhat from each other. The latter difference insofar as energy loss by ionization alone is considered is not a large per cent for energies of 1 to 3 Bev.)

Thus, we are lead to the probable conclusion that at least three-fourths of the protons found at 30,000 ft above sea level are of secondary origin. The remaining protons may well come directly from a primary proton component.

REFERENCES

1. W. Gentner, H. Maier-Leibnitz, W. Bothe, Atlas Typischer Nebelkammerbilder, Julius Springer, Berlin, 1940
2. C. R. Skobelzyn, Z. Phys., 54, 686 (1929)
3. Carl D. Anderson, Phys. Rev., 41, 405 (1932)  
Carl D. Anderson, Phys. Rev., 44, 5 (1933)  
Carl D. Anderson and Seth H. Neddermeyer, Papers and Discussions of the International Conference on Physics, London 1934, Vol. I, p. 171, University Press, Cambridge
4. P. Kunze, Z. Phys., 80, 559 (1933)
5. P. M. S. Blackett, Proc. Roy. Soc., A159, 1 (1937)
6. L. LePrince-Ringuet and Grussard, J. Phys. Radium, 8, 207 (1937)
7. H. Jones, Rev. Mod. Phys., 11, 235 (1939)
8. D. J. Hughes, Phys. Rev., 57, 592 (1940)
9. W. M. Powell, Phys. Rev., 69, 385 (1946)
10. G. Herzog and W. H. Bostick, Phys. Rev., 59, 117, 122 (1941)
11. H. A. Bethe, Phys. Rev., 70, 821 (1946)
12. M. Blau and H. Wambacher, Nature, Lond., 140, 585 (1937)
13. A. Widhalm, Z. Phys., 115, 481 (1940)
14. W. Heisenberg, Cosmic Radiation, Dover Publications, New York (1946) p. 8
15. L. W. Nordheim, Phys. Rev., 56, 502 (1939)

16. M. Schein, W. P. Jesse, and E. O. Wollan, Phys. Rev., 59,  
930 (1941)
17. I. Bloch, Phys. Rev., 69, 575 (1946)
18. G. Herzog and P. Scherrer, Helv. Phys. Acta, 8, 514 (1935)

APPENDIX A

Measurements of cosmic ray energies which have been made by several investigators are discussed below.

In 1932 and 1933 Anderson reported measurements on the energies of random cosmic ray particles. In 1934 Anderson and Neddermeyer<sup>(3)</sup> reported a determination of the sea level spectrum for counter-controlled tracks only. Table V and Figs. 10 and 11 show these data. This energy distribution is based on a relatively small number of tracks which showed little distortion. All rays were considered to be directed downward for the determination of the sign of charge of the particles. Curvature measurements were made on the original film using a method similar to that described in Appendix C. The following facts are evident from the data: (1) the numbers of particles decrease with increasing energies, (2) positive and negative particles occur in about the same numbers, there being a small positive excess, and (3) subject to considerable statistical uncertainty, the data show similar distribution curves for positive and negative particles. All the particles in the reported spectrum were interpreted as electrons. Since the discovery of the mesotron, single particles at sea level are believed to be mesotrons.

TABLE V Sea Level Data of Anderson and Neddermeyer

Energy in Million Electron-Volts for Each Particle

<u>Positive Particles</u>	<u>Negative Particles</u>
310	1500
350	1600
400	1700
420	1800
560	2300
700	2500
730	2500
780	2700
780	2700
780	2800
850	3200
930	3300
980	3600
1000	3700
1100	3900
1200	4600
1350	5000
1500	5900
1500	
1600	
1600	

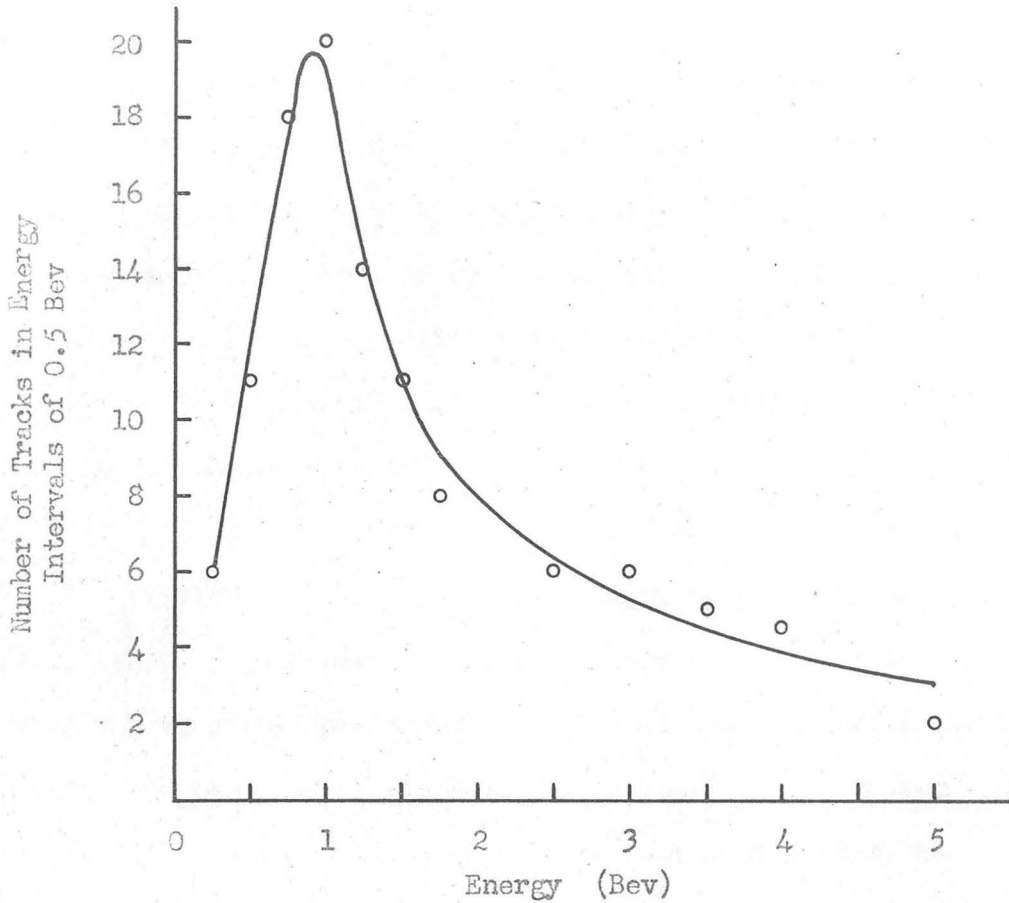


Fig. 10 Spectrum of All Particles (Anderson)

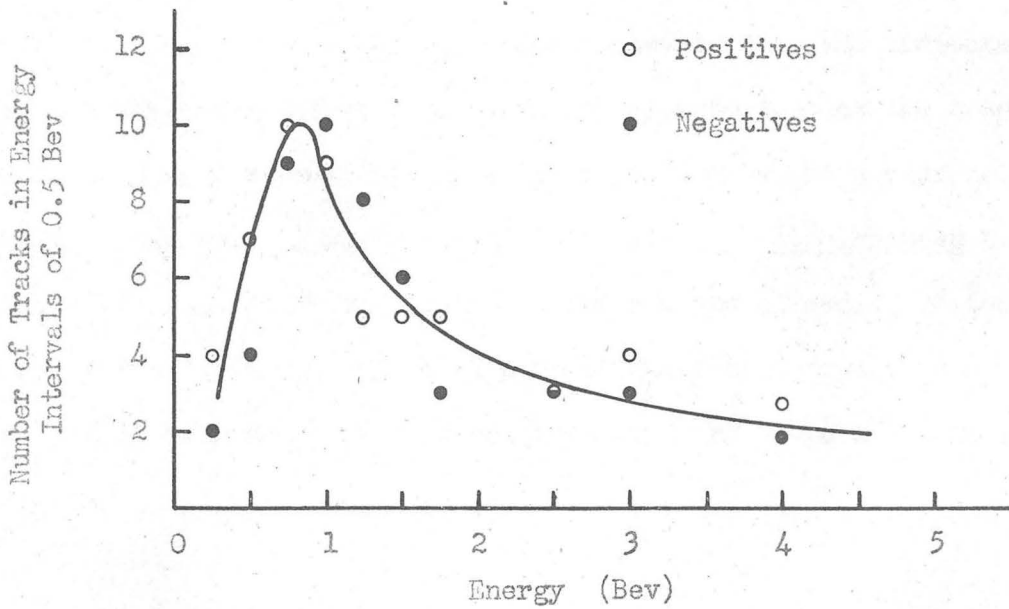


Fig. 11 Spectra of Positive and Negative Particles (Anderson)

The sea level data of Kunze (1933)<sup>(4)</sup> agrees essentially with the random particle spectra of Anderson. Kunze used a 16-cm chamber in a magnetic field of 18,000 gauss, and reported measurements of momenta valid up to about  $10^7$  gauss-cm. Kunze referred to all positive particles as "protons" but recognized difficulties in so identifying them. (The announcement of the discovery of the positron is dated September, 1932.)

Blackett's investigation,<sup>(5)</sup> reported in 1937, was perhaps the most painstaking research on the energy spectrum carried out up until that time. He reported measurements on 829 single tracks obtained with a magnetic field of 12,000 gauss. In order to measure accurately such a large number of tracks, he introduced a novel method of measurement. The track was projected onto a screen. Into the optical system was introduced a parallel glass plate, which on rotation produced curvature in the projected track. When the added curvature was opposite to that of the track the latter could be made to appear straight. Thus the measurement technique was reduced to a determination of track straightness by oblique observation of the projected image, and a reading of the scale of the calibrated parallel plate. Curvatures from 0 to  $3 \text{ m}^{-1}$  could be measured with a probable error of  $0.016 \text{ m}^{-1}$ .

Blackett's data are reproduced in Figs. 12, 13, and 14. The distribution curves are given in terms of "energies" defined as 300 Hp. According to the author these measurements "have considerable validity up to about, say, 10 Bev, a small validity up to 20 Bev, and none at all for higher energies."

The following conclusions are found: (1)  $53 \pm 2$  per cent of the particles are positive,  $47 \pm 2$  per cent are negative -- i.e., about equal numbers of positive and negative particles are present; and (2) both positive and negative curves are quite similar, each having a maximum at about 1 Bev with decreasing numbers of particles for higher energies.

Blackett discusses in some detail the possible significance of the "fine-structure" apparent in the curves (Figs. 12 to 14) in the energy range 2 to 4 Bev. He concludes that this structure probably is real although he recognized that there is a small possibility that the effect is of statistical origin.

None of Blackett's sea level particles could with certainty be identified as a proton, although 3 tracks in a total of 1500 might have been proton tracks. This almost complete absence of protons among sea level cosmic rays is consistent

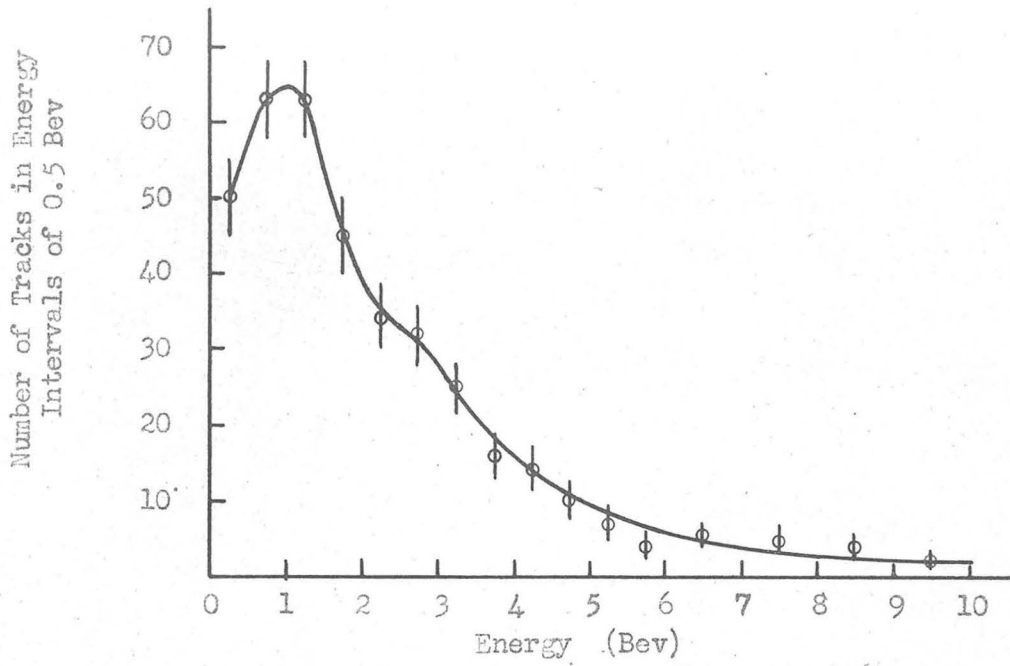


Fig. 12 Spectrum of Positive Particles (Blackett)

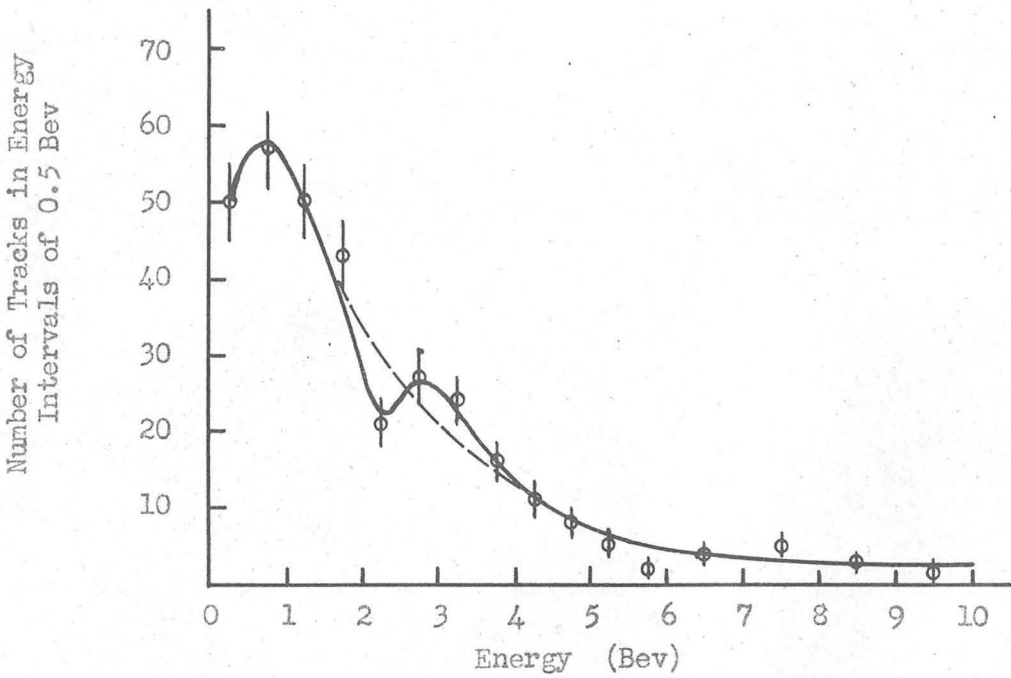


Fig. 13 Spectrum of Negative Particles (Blackett)

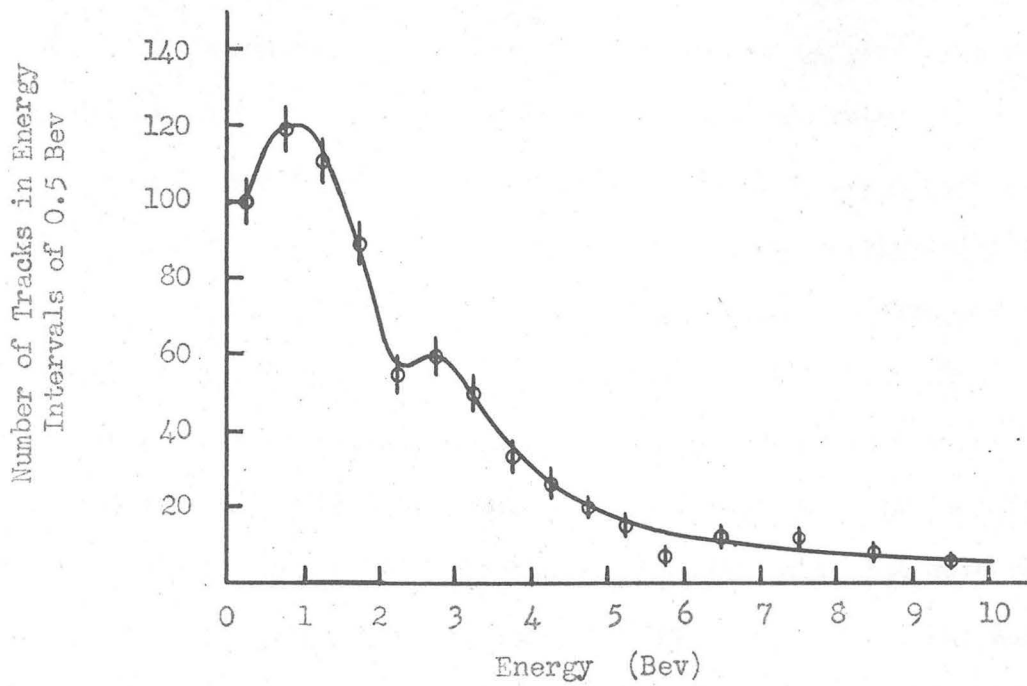


Fig. 14 Spectrum of All Particles (Blackett)

with the findings of Anderson and of others.

Leprince-Ringuet and Crussard reported in 1937<sup>(6)</sup> the results of sea level energy measurements using a field of 13,000 gauss and the following arrangements: (A) two Geiger tubes below the cloud chamber, (B) the same arrangement of Geiger tubes as in A, but with 14 cm of lead interposed between the tubes, and (C) two Geiger tubes with 14 cm of lead between them placed above the chamber. The arrangement A produced data which show similar positive and negative spectra with a very small positive excess, in the "energy" range 1 to 10 Bev. The statistical uncertainties are too great to confirm or deny the fine-structure of Blackett's spectra in the 2 to 4 Bev range. The arrangement B resulted in a positive spectrum similar to that of A except that the numbers of particles are decreased for energies less than 4 Bev. The negative spectrum, however, shows a decrease for all energies and thus there appears a positive-to-negative particle ratio of 1.7. There appears a larger percentage of particles which are not deviated by the magnetic field. Arrangement C resulted in similar positive and negative spectra, the principal difference between the results of arrangements B and C being a shift of some of the very high energy particles (non-deviated rays) into the negative spectrum. The fact that the Geiger tube arrangement of C differs from that of A and B probably affects the relative distributions.

Other sea level energy distributions were reported by Jones (1939)<sup>(7)</sup> and Hughes (1940).<sup>(8)</sup> These investigators used the same 30-cm chamber with magnetic fields of 12,000 to 16,000 gauss. These experiments employed three Geiger tubes -- two above the chamber and one below. Spectra with and without a 10-cm lead absorber between the chamber and the bottom tube were made. Approximately 600 particles are included in each experiment. A positive excess of about ten per cent of the total number of particles is found whether the lead is present or not. The positive excess is distributed throughout the spectrum, which covers the "energy" range 0.5 to 10 Bev. The only apparent difference between the spectra obtained without and with lead is the absorption in the latter case of particles of low energy (less than 200 Mev). These results seem to be at variance with those of Leprince-Ringuet. The experimental arrangement in the latter case is, however, different, so that a direct comparison may have questionable validity.

There seem to be no published magnetic curvature determinations of the cosmic ray spectra at altitudes of the order of 14,000 ft. Herzog and Scherrer (1935)<sup>(18)</sup> reported that energy measurements had been made on 383 tracks obtained in a magnetic field of 2500 gauss at an altitude of 3540 m, but this article fails to give curves or tables of data. The upper limit on the

energy measurements is stated to be 50 Mev.

W. M. Powell reported in 1946<sup>(9)</sup> cloud chamber experiments in which energies were determined by the measurement of the ranges of particles in lead plates placed inside the chamber. A distribution of energies is not reported, but data on mesotrons and protons are discussed in the article. The two types of particles are distinguished from each other (and from electrons) by a method involving the ionization, and the scattering in lead plates. It was found that the particles identified as mesotrons fall off in numbers with increasing energies in the same proportion that other penetrating particles do, penetrating particles being defined to be those which traverse more than two plates without producing secondaries. Protons are reported to be most abundant at lower energies with very few of energies as great as 200 Mev present. Powell interprets this result as a "dying out (of protons) at energies around 200 Mev." He postulates that the small number of high energy protons is due to a large cross-section for the production of mesotron-pairs by the higher energy particles.

Hertzog and Bostick reported in 1941<sup>(10)</sup> the results of one flight to 29,000 ft in a DC-3 transport plane with a cloud chamber having a magnetic field of 700 gauss. The authors state that in 155 pictures "51 slow mesotrons and 39 proton tracks were

identified." In view of the fact that a magnetic field of 700 gauss is practically negligible when applied to momentum measurements of mesotrons and protons, these data cannot have quantitative meaning, nor even much qualitative meaning. It may be further remarked that the results reported by Hertzog and Bostick are not confirmed by the present experiments.

#### APPENDIX B

Figs. 15, 16, 17, and 18 show diagrams of the electronic control equipment. The circuits are rather conventional, so that the diagrams are largely self-explanatory.



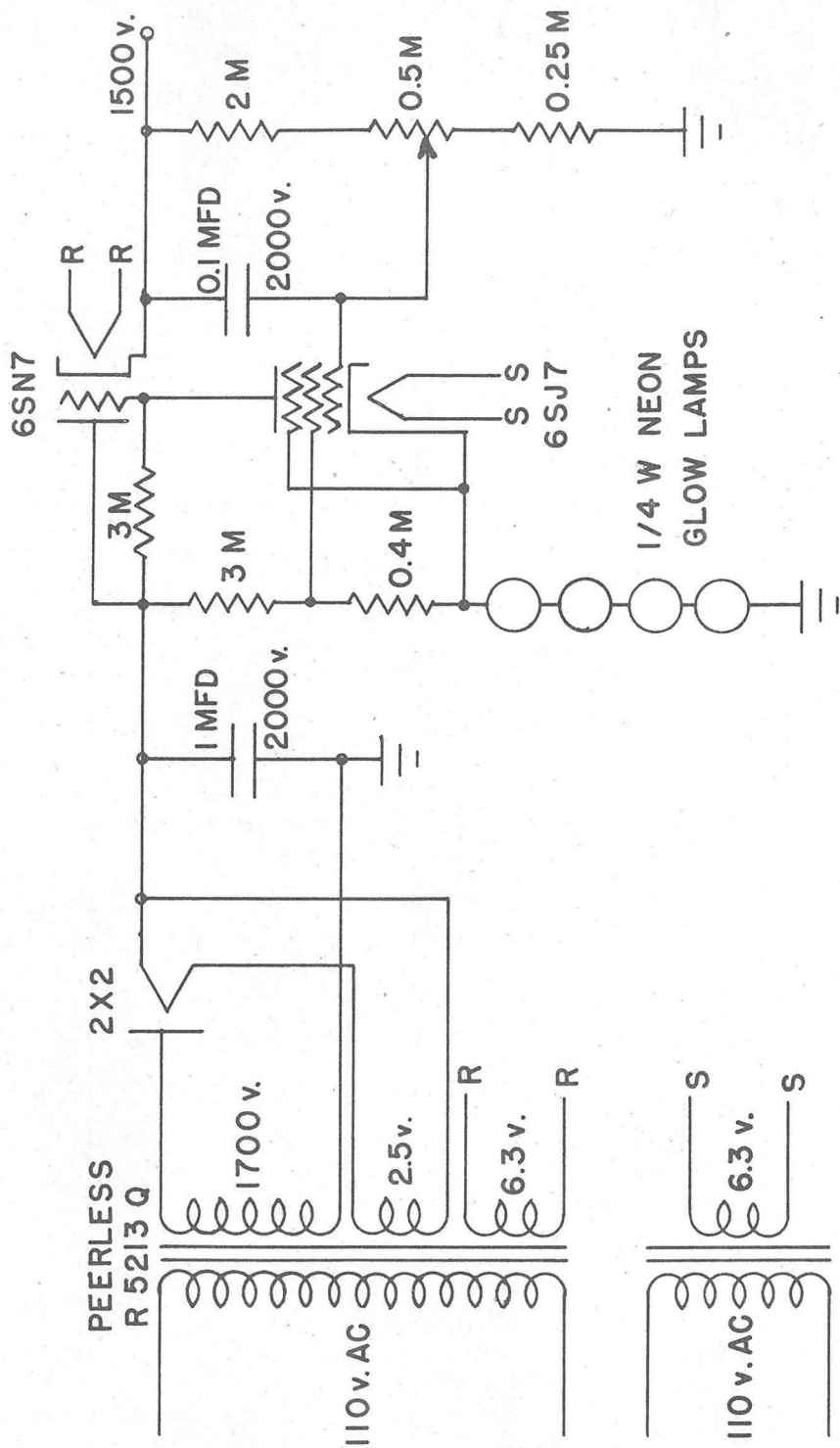


Fig. 16 Electronic Control Equipment -- High Voltage Power Supply

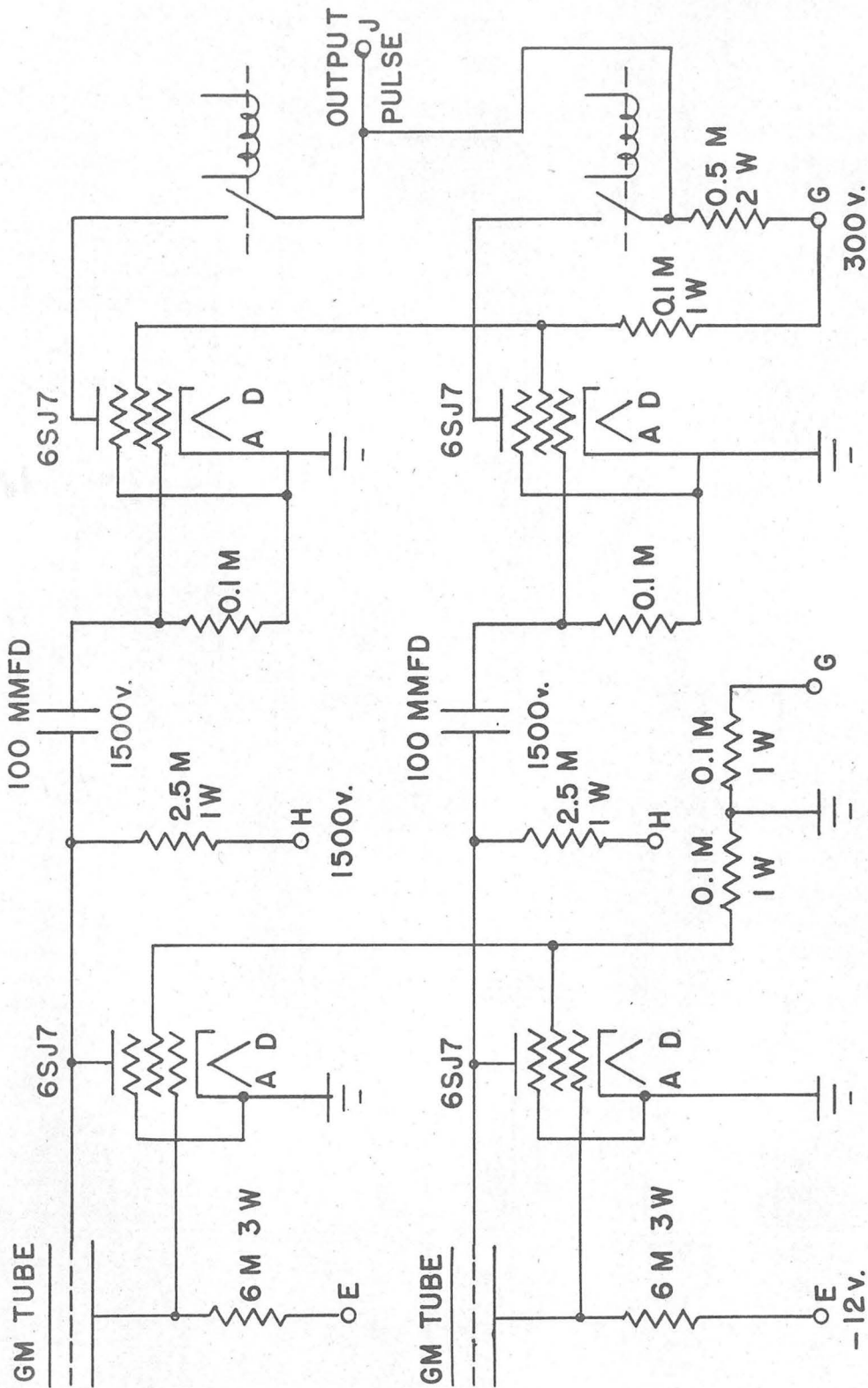


Fig. 17 Electronic Control Equipment -- Neher-Harper and Rossi Circuits

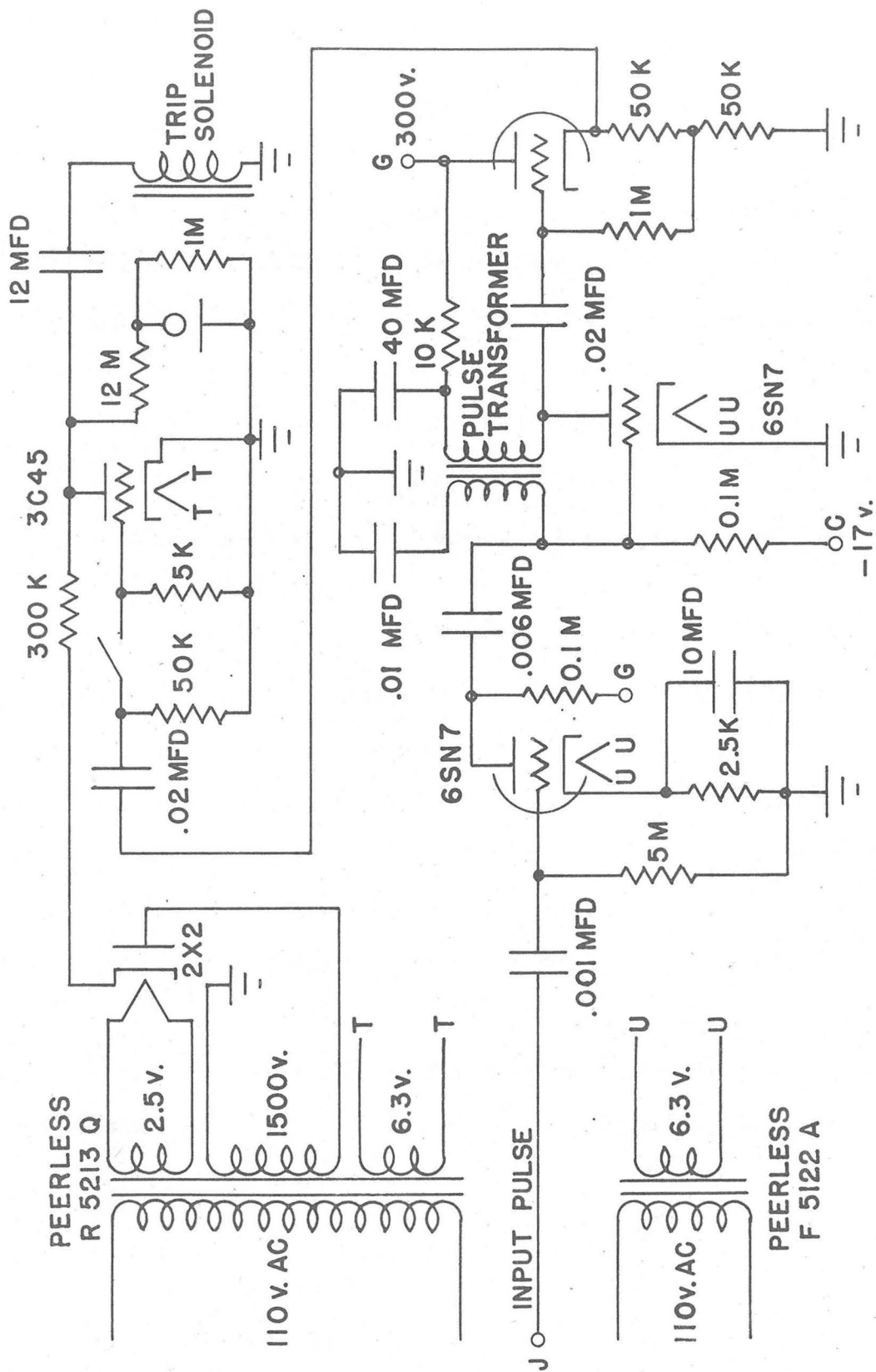


Fig. 18 Electronic Control Equipment --- Pulse Amplifier and Trip Circuit

APPENDIX C

Tracks having radii of curvature greater than 140 cm are measured with a comparator. The comparator permits measurements of position to an accuracy of  $10^{-3}$  cm in the vertical (y) direction and to an accuracy of  $10^{-4}$  cm in the horizontal (x) direction. In practice, the horizontal coordinates of position can be measured only to an accuracy of about 1/2000 of a centimeter, the limitation being in the film image rather than in the comparator.

Measurements are made on the original film, which is placed in the comparator with the track parallel to the vertical direction. The x-coordinates are determined for successive points whose y-coordinates differ by 0.1 cm. Thus the number of coordinates determined for each track lies between 12 and 20, depending upon the track lengths, which vary from 8 cm to 15 cm.

From ten to twenty minutes are required to measure each track, the time depending upon the quality of the film and the skill of the observer.

The measurements are plotted on coordinate paper. A suitable magnification for the y-axis is 0.1 cm on the film

equals 1.0 cm on the graph. The corresponding x-axis magnification to be used depends upon the degree of curvature of the track. Magnifications of 0.001, 0.002, 0.004, and 0.005 cm, respectively, on the film equal to 1.0 cm on the graph are used.

It is well known that the path of a charged particle, moving with constant velocity in a uniform magnetic field, is an arc of a circle. The analytic equation of a circle of radius  $\rho$  whose center is on the x-axis and whose arc passes through the origin of coordinates is

$$(x - \rho)^2 + y^2 = \rho^2$$

If the x-coordinates are transformed by the equation,  $x' = ax$ , the equation for the circle becomes (dropping the prime):

$$(x - a\rho)^2 + (ay)^2 = (a\rho)^2$$

This will be recognized as the equation of an ellipse of major axis  $a\rho$  and minor axis  $\rho$ , with center at  $x = a\rho$ . The equation can also be written:

$$x = \frac{ay^2}{2\rho} \left[ 1 + \left( \frac{x}{ay} \right)^2 \right]$$

If this be expanded in a power series in  $y$ , then

$$X = \frac{ay^2}{2\rho} \left[ 1 + \left(\frac{y}{2\rho}\right)^2 + \text{higher order terms} \right]$$

The error introduced into the values of  $x$  by neglecting the squared term will be about 0.1 per cent for a track 15 cm long and of radius 140 cm. For straighter tracks the error will be less. (This error is, of course, an order of magnitude smaller than other errors entering into the data.)

The remaining equation will be recognized as that of a parabola:

$$X = \frac{ay^2}{2\rho}$$

Thus, the plotted coordinates of positions along a track should fall on a smooth curve which is a parabola. A family of parabolas drawn on transparent paper can be compared with the plotted data to determine which parabola is the best fit.

When the cloud track is not accurately aligned in the comparator, the coordinate plot shows a parabola with unequal arms. When this assymetry is very pronounced, it is desirable to re-plot the graph by the method indicated in Fig. 19 before

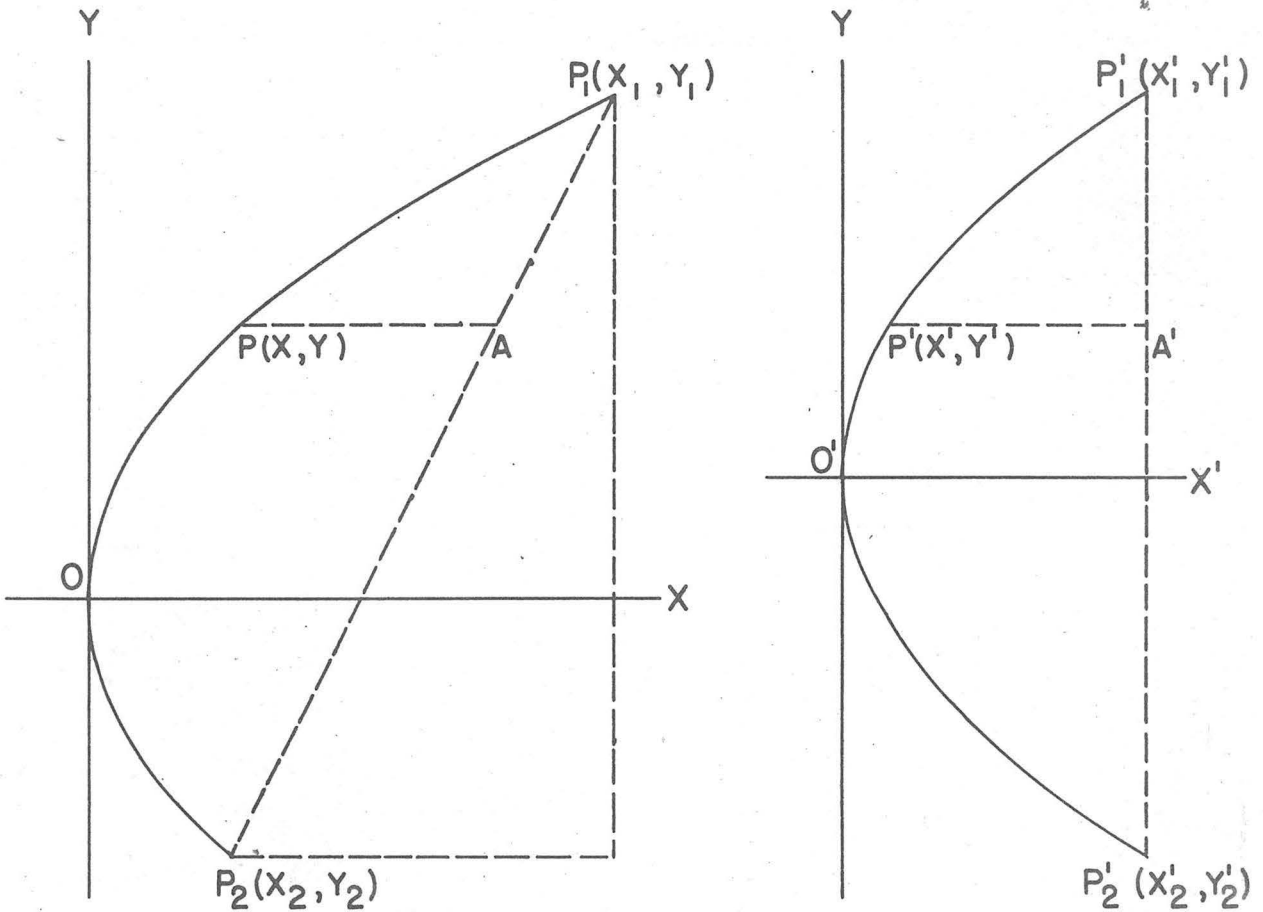


Fig. 19 Graphical Method for Transformation of Asymmetrical Parabola into Symmetrical Parabola

Draw  $P_1P_2$ , connecting the end points of the parabola. Draw a line  $P'_1P'_2$  parallel to the y-axis and of length  $(y_1 - y_2)$ . For each point  $P(x, y)$  on the first parabola locate the corresponding point  $P'(x', y')$  on the new parabola by making  $P'A'$  equal  $PA$ , and  $P'_1A'$  equal to the projection on the y-axis of  $P_1A$ . Each parabola will be an arc of the same parabolic curve.

an attempt is made to fit a parabola to the points. This is equivalent to performing the transformation:

$$\bar{y} = y - \frac{1}{2} (y_1 + y_2)$$

$$\bar{x} = x - x_1 + \frac{a}{2p} (y_1 + y_2)(y_1 - y)$$

where  $x_1 = \frac{a}{2p} y_1^2$  ; and  $x_2 = \frac{a}{2p} y_2^2$

These equations transform the parabola

$$x = \frac{a}{2p} y^2 \quad \text{into the parabola} \quad \bar{x} = \frac{a}{2p} \bar{y}^2$$

The new curve is seen to be but a different segment of the same parabolic curve.

When the parabola which fits the plotted points of the track has been found, the magnetic curvature,  $H\rho$ , can be computed. It is convenient to prepare for a given magnetic field strength a table which gives directly the magnetic curvature as a function of the parabola number and the plotting magnification. The magnetic curvature of a track is given by

$$H_p = H \left( \frac{M_1}{M_2} \right) \left( \frac{a}{2} \right) \frac{y^2}{x}$$

where x and y are any two corresponding coordinates on that parabola which fits the plotted points,  $M_1$ , equals 7.4, is the ratio of the "life" size of the track to its image size on the film,  $M_2$  is the magnification of the plotted y-coordinates over the measured coordinates on the film, and  $a$  (as above) is the ratio of the magnification of the plotted x-coordinates to that of the plotted y-coordinates.

For sharp tracks the accuracy of magnetic curvature measurements is limited principally by the distortion produced in the tracks by motion of the gas within the cloud chamber. Examination of many plots of tracks is necessary for the determination of the type and magnitude of the distortion. Occasionally, one or two points on a plot may, for statistical reasons, be out of position in a way that makes the track appear to take a sharp bend at those points. Misinterpretation of such data is avoided by a final inspection of the projected photograph of the track. By looking obliquely along the image of the track, one can determine whether apparent distortions indicated in the plotted track are real.

Fig. 20 shows the plot of a track of relatively large curvature; it appears to have little distortion. In Fig. 21 is shown the plot of a representative track of medium energy, which shows statistical deviation from the curve of a parabola as well as some local distortion. (The magnifications for Figs. 20 and 21 are different.) For such a track it may be that several neighboring parabolas in the family of test curves fit the plotted points equally well. If this is true, the middle parabola is chosen as the best fit, and the extreme parabolas give the outside limits of error. If this error affects the magnetic curvature by more than ten per cent, then it is the principal source of error. Fig. 22 shows a track of very high momentum, which is still measurable but only within rather large error limits. Fig. 23 shows the plot of a track for which only a lower momentum limit can be set. The lower limit is determined by that parabola which gives a reasonable fit to the plotted points when it is concave to the right as well as to the left; that is to say, a "straight" track can be taken to be slightly curved in either direction due to the fact that the measured points scatter about a straight line.

The estimated errors to be expected for various momenta are given in Section IV.

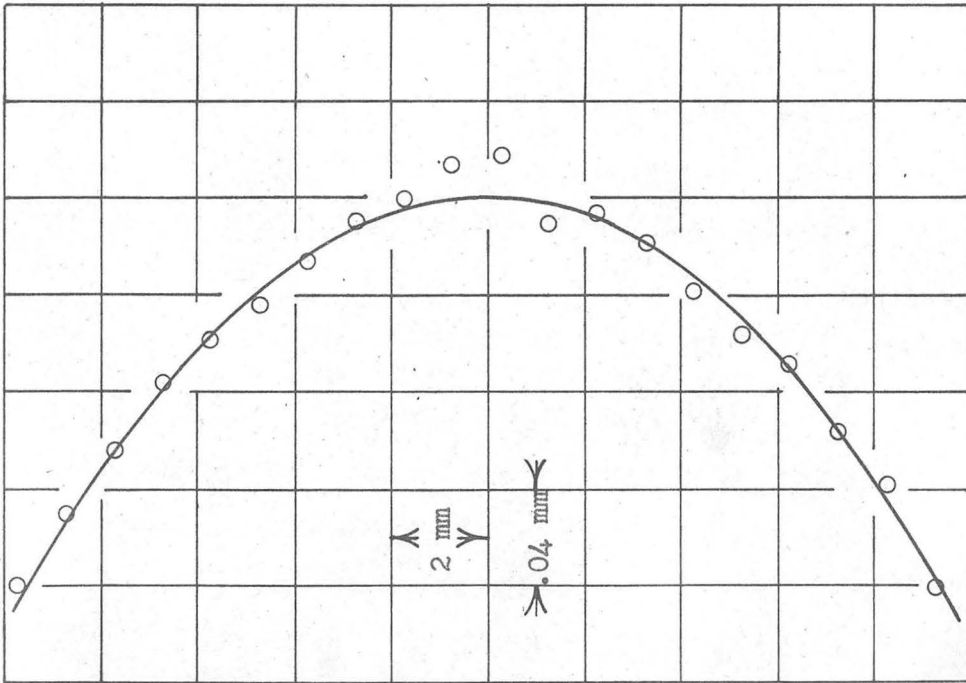


Fig. 20 This is the plot of the proton track of Fig. 1. Measurement accuracy is better than 10 per cent. ( $H_p = 1.6 \times 10^6$  gauss-cm. Scale is  $1/7.4$  of life size.)

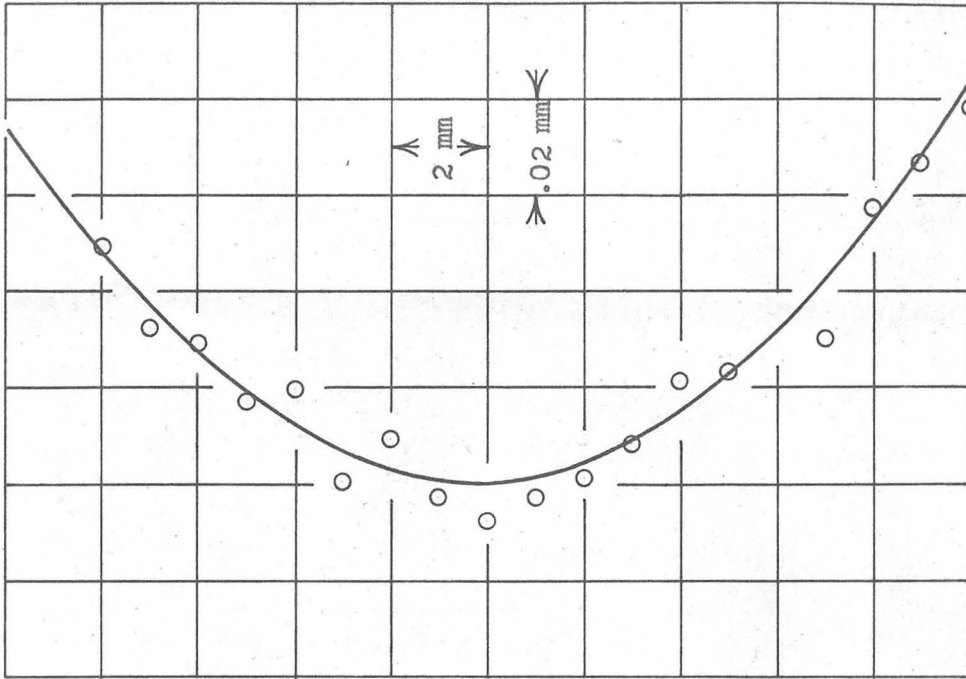


Fig. 21 This is the plot of a representative track of medium energy. Measurement accuracy is about 15 per cent. ( $H_p = 3.8 \times 10^6$  gauss-cm. Scale is  $1/7.4$  of life size.)

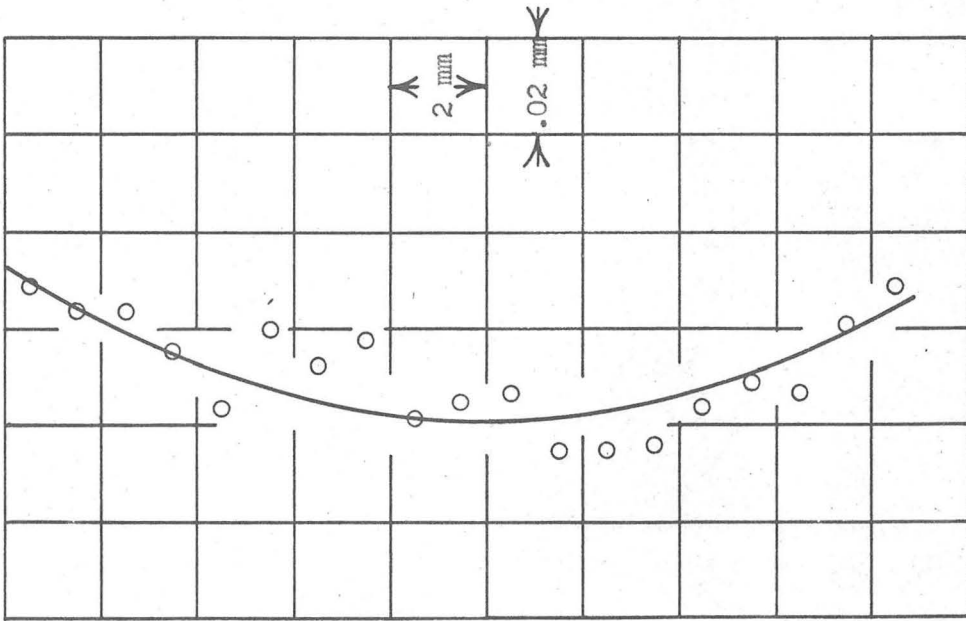


Fig. 22 This is the plot of a high energy track. Measurement accuracy is about 50 per cent. ( $H_p = 9 \times 10^6$  gauss-cm. Scale is  $1/7.4$  of life size.)

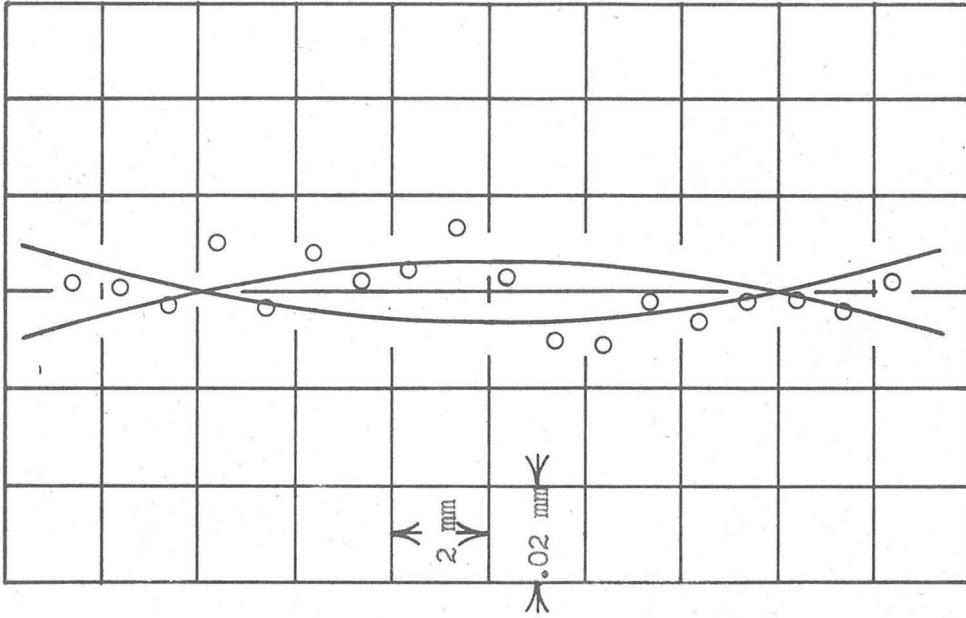


Fig. 23 This is the plot of a very high energy track, for which only a lower energy limit can be determined. ( $H_p > 1.5 \times 10^7$  gauss-cm. Scale is  $1/7.4$  of life size.)